Young Investigator's Award, 8th World Biomaterials Congress, Amsterdam RAI, The Netherlands, May 28–June 1, 2008

In vivo evaluation of a multiphased scaffold designed for orthopaedic interface tissue engineering and soft tissue-to-bone integration

Jeffrey P. Spalazzi,[1] Elias Dagher,[2] Stephen B. Doty,[3] X. Edward Guo,[4] Scott A. Rodeo,[2] Helen H. Lu[1,5]
[1]*Biomaterials and Interface Tissue Engineering Laboratory, Department of Biomedical Engineering, Columbia University, New York, New York 10027*
[2]*Soft Tissue Research Laboratory, Hospital for Special Surgery, New York, New York 10021*
[3]*Analytical Microscopy Core Laboratory, Hospital for Special Surgery, New York, New York 10021*
[4]*Bone Bioengineering Laboratory, Department of Biomedical Engineering, Columbia University, New York, New York 10027*
[5]*College of Dental Medicine, Columbia University, New York, New York 10032*

Received 18 January 2008; accepted 12 March 2008
Published online 28 April 2008 in Wiley InterScience (www.interscience.wiley.com). DOI: 10.1002/jbm.a.32073

Abstract: Achieving functional graft integration with subchondral bone poses a significant challenge for orthopaedic soft tissue repair and reconstruction. Soft tissues such as the anterior cruciate ligament (ACL) integrate with bone through a fibrocartilage interface, which minimizes stress concentrations and mediates load transfer between soft and hard tissues. We propose that biological fixation can be achieved by regenerating this fibrocartilage interface on biological or synthetic ACL grafts. This study focuses on the *in vivo* evaluation of a stratified scaffold predesigned to mimic the multitissue transition found at the ACL-to-bone interface. Specifically, the scaffold consists of three distinct yet continuous phases: Phase A for ligament formation, Phase B for the interface, and Phase C for the bone region. Interface-relevant cell types, specifically fibroblasts, chondrocytes, and osteoblasts, will be tri-cultured on this scaffold, and the formation of cell type- and phase-specific matrix heterogeneity as well as fibrocartilage formation will be evaluated over 8 weeks in a subcutaneous athymic rat model. Acellular scaffolds as well as scaffolds co-cultured with fibroblasts and osteoblasts will serve as controls. It was found that the triphasic scaffold supported multilineage cellular interactions as well as tissue infiltration and abundant matrix production *in vivo*. In addition, controlled phase-specific matrix heterogeneity was induced on the scaffold, with distinct mineral and fibrocartilage-like tissue regions formed in the tri-cultured group. Cell seeding had a positive effect on both host infiltration and matrix elaboration, which also translated into increased mechanical properties in the seeded groups compared to the acellular controls. In summary, the biomimetic and multiphasic design coupled with spatial control of cell distribution enables multitissue regeneration on the stratified scaffold, and demonstrates the potential for regenerating the interface between soft tissue grafts and bone. © 2008 Wiley Periodicals, Inc. J Biomed Mater Res 86A: 1–12, 2008

Key words: biological fixation; multi-phased scaffold; tri-culture; co-culture; insertion; anterior cruciate ligament; interface tissue engineering

Correspondence to: H. H. Lu; e-mail: hl2052@columbia.edu
Contract grant sponsor: NIH/NIAMS; contract grant number: R21 AR052402 (HHL)
Contract grant sponsor: NSF Graduate Fellowship; contract grant number: GK-12 0338329
Contract grant sponsors: Wallace H. Coulter Foundation (HHL/SAR), Columbia University Science and Technology Ventures Seed Grant (HHL)

INTRODUCTION

The anterior cruciate ligament (ACL) is the most frequently injured ligament of the knee,[1] with ~100,000 reconstruction procedures performed annually in the United States.[2,3] Because of its inherently poor healing potential and limited vascularization, ACL ruptures do not heal and reconstruction surgery is required to restore joint function.[4–6]

Autogenous bone-patellar tendon-bone and hamstring tendon grafts are commonly used for ACL reconstruction. The hamstring tendon-based grafts, which include the gracilis and/or semitendinosus tendons, are increasingly utilized clinically due to the high incidence of donor site morbidity associated with harvesting bone-patellar tendon-bone grafts.[7,8] Over the past decade, improved fixation options such as transfemoral pins have helped to secure the hamstring graft, permitting the utilization of the superior biomechanical properties of these grafts while reducing the iatrogenic complications associated with bone-patellar tendon-bone graft harvest. However, the primary factor limiting clinical success and prevalent application of hamstring tendon grafts remains their inability to achieve biological fixation with subchondral bone.[9–11]

The ACL, similar to many other ligaments and tendons with direct insertions, transitions into bone through a characteristic fibrocartilage interface, with controlled spatial variations in cell type and matrix composition.[12–22] It is well documented that three distinct and continuous tissue regions exist at the insertion: ligament, fibrocartilage, and bone. The fibrocartilage region is further divided into noncalcified and calcified fibrocartilage zones. It is postulated that this controlled matrix heterogeneity permits a gradual transition of loading between soft tissue and bone, and in turn minimizes the formation of stress concentrations at the interface between soft and hard tissues.[13,23] While ACL grafts may restore joint function through mechanical fixation, this multitissue insertion is not re-established following reconstruction surgery. Without an anatomical interface, the graft-bone junction has limited mechanical stability,[9–11] and this lack of functional integration remains the primary cause of graft failure.[10,11,24–26] Therefore, regeneration of the multi-tissue interface will be critical for soft tissue-to-bone fixation.[27,28]

To recapitulate the complex multi-tissue organization inherent at the ACL-to-bone junction, multiple types of cells, a scaffold system which supports interactions between these different cell types, and the development of distinct yet continuous multitissue regions mimicking the organization of the native insertion site will be required. Therefore, in addition to supporting the growth and differentiation of relevant cell types, the ideal scaffold for interface tissue engineering must direct heterotypic and homotypic cellular interactions while promoting the formation and maintenance of controlled matrix heterogeneity. Consequently, the scaffold should exhibit a gradient of structural and material properties mimicking those of the native insertion site. Compared to a homogenous structure, a scaffold with predesigned inhomogeneity may better sustain and transmit the distribution of complex loads inherent at the ACL-to-bone interface.[29,30] The interface scaffold must also be biodegradable and exhibit mechanical properties comparable to those of the ligament insertion site. Finally, in order to promote *in vivo* graft integration, the tissue engineered graft must be utilized with current ACL reconstruction grafts or preincorporated into the design of ligament replacement grafts.

Recently, we reported on the design of a multiphased scaffold for interface tissue engineering.[31] Specifically, the scaffold consisted of three distinct yet continuous phases [Fig. 1(A)], with each designed for a particular cell type and tissue region found at the interface: Phase A for fibroblasts and soft tissue formation, Phase B as the interface region intended for fibrochondrocytes and fibrocartilage formation, and Phase C for osteoblasts and bone tissue. *In vitro* evaluation of fibroblast-osteoblast co-culture demonstrated that the stratified scaffold design enabled spatial control of cell distribution, with both osteoblasts and fibroblasts localized in their respective regions, while restricting their interaction to the interface region. This controlled cell distribution also resulted in the formation of cell type-specific matrix on each phase, with an extensive type I collagen matrix found on both Phases A and B, and a mineralized matrix detected only in Phase C. These findings demonstrate the feasibility of engineering regional tissue heterogeneity *in vitro* on a stratified scaffold with biomimetic matrix organization.

Building upon these promising *in vitro* results, the objectives of the current study were three-fold. The first objective was to investigate whether the phase-specific distribution of distinct tissue regions observed on the co-cultured triphasic scaffold *in vitro* would be maintained *in vivo*. Specifically, fibroblast and osteoblast co-culture on the triphasic scaffold was evaluated *in vivo* using a subcutaneous athymic rodent model. Currently, in both 2D and 3D co-culture models of fibroblasts and osteoblasts,[31,32] while gene expression of fibrocartilage-related markers has been reported, no fibrocartilage-like tissue has been formed in the interface region. Therefore, the second study objective was to expand the co-culture system to triculture of fibroblasts, chondrocytes, and osteoblasts in order to evaluate the potential for developing a fibrocartilage interface-like region directly on the triphasic scaffold. As part of the scaffold optimization, the third study objective was to determine the effect of the *in vivo* environment and cell preseeding on scaffold mechanical properties and structural integrity over time. This is the first reported study to investigate the development of distinct matrix zones mimicking the ligament-to-bone interface on a single construct *in vivo*. It was anticipated that by exerting spatial control of the distribution of the interface-relevant cell populations in co-culture and tri-culture on the

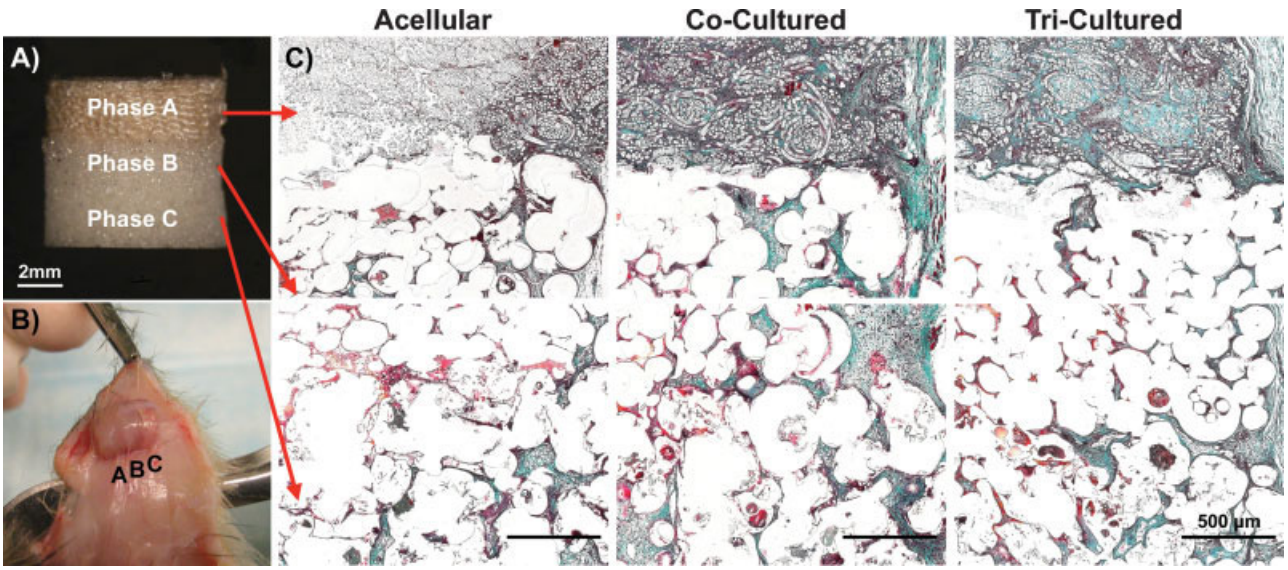

Figure 1. Host Tissue Infiltration into the Multi-Phased Scaffold. (A) Triphasic scaffold with three distinct yet continuous phases: Phase A for soft tissue formation, Phase B for interface formation, and Phase C for bone formation. (B) Explanted tri-cultured scaffold, week 4. (C) Collagen production (green) in the dorsal side of the acellular, co-cultured, and tri-cultured scaffolds after 4 weeks of implantation. Tissue infiltration and extracellular matrix production were more extensive in the co-cultured and tri-cultured groups than the acellular control. (Modified Goldner's Masson Trichrome, week 4, 5×, bar = 500 µm).

triphasic scaffold, both cell type- and phase-specific matrix formation would be developed *in vivo*. From a broader perspective, multitissue regeneration through multiphasic scaffold design and controlled cellular interactions represents a promising strategy for achieving biological fixation of tissue engineered ACL grafts, with the potential to facilitate the development of complex musculoskeletal tissue or organ systems.

MATERIALS AND METHODS

Scaffold fabrication

A stratified scaffold with three distinct yet continuous phases [Fig. 1(A)] was fabricated.[31] Phase A was formed from polyglactin 10:90 knitted mesh sheets (Vicryl VKML, Ethicon, Somerville, NJ) by sintering layers of the polymer mesh in cylindrical molds at 150°C for 20 h. Phase B consisted of poly(D,L-lactic-*co*-glycolic acid) 85:15 copolymer (PLGA, $M_w \approx 123.6$ kDa, Alkermes, Cambridge, MA) microspheres formed via a water/oil/water emulsion.[33,34] Briefly, PLGA (10% w/v) was first dissolved in dichloromethane (EM Science, Gibbstown, New Jersey), then mixed with a 1% poly(vinyl alcohol) solution (Sigma Chemicals, St. Louis, MO) to form polymer microspheres. The microspheres were then sintered at 55°C for 5 h to form Phase B. The third phase (Phase C) was comprised of composite microspheres[31,34] with a 4:1 ratio of PLGA and 45S5 bioactive glass (BG, 20 µm, MO-SCI Corporation, Rolla, MD). The PLGA-BG microspheres were sintered at 55°C for 5 h to form Phase C.

To fabricate the triphasic scaffold, Phases A and B were first integrated via organic solvent and subsequently sintered onto Phase C by heating all three phases for 10 h at 55°C.[31] The triphasic scaffolds were sterilized with ethylene oxide and vacuum desiccated for 24 h prior to cell seeding. Total scaffold diameter ($n = 70$) and thickness ($n = 70$) were measured using a digital caliper. The post-fabrication diameter of each phase was 6.9 ± 0.2 mm, 7.5 ± 0.1 mm, and 7.50 ± 0.01 mm, respectively, and the thicknesses of Phases A, B, and C were 2.3 ± 0.1 mm, 2.7 ± 0.2 mm, and 2.6 ± 0.2 mm, respectively. Scaffold phase integrity was ascertained by scanning electron microscopy (3 kV, JEOL 5600LV, Tokyo, Japan and FEI Quanta 600, FEI Company, Hillsboro, OR),[31] and porosity was characterized by mercury porosimetry (Micromeritics, Norcross, Georgia).[31] The above fabrication protocol consistently results in a triphasic scaffold with a porosity of 58 ± 5%, 34 ± 4%, and 32 ± 1% in Phases A, B, and C, respectively.

Cells and cell culture

Primary neonatal bovine (1 to 7 day old calves) fibroblasts and osteoblasts were obtained respectively from explant cultures of ACL and cortical bone tissue following published methods.[35,36] For the fibroblast cultures, the ligament tissue was minced and incubated in fully supplemented DMEM, and cell migration from the explants was monitored. Only cells derived from the second migration were used in order to ensure a relatively homogenous cell population.[32,35] For osteoblast outgrowth, cortical bone chips were isolated from bovine tibiae using a bone ronguer. The bone chips were first rinsed thoroughly with phosphate-buffered saline (PBS, Sigma Chemicals, St.

Louis, MO) to remove the bone marrow, then cultured in Dulbecco's Modification of Eagle's Medium (DMEM) supplemented with 10% fetal bovine serum (Atlanta Biologicals, Atlanta, GA), 1% nonessential amino acids, and 1% penicillin/streptomycin. For chondrocyte cultures, the primary bovine chondrocytes were isolated from knee articular cartilage by collagenase digestion (Worthington Biochemical Corp., Lakewood, NJ).[37–39] Chondrocytes were plated for 3 days prior to scaffold seeding. The respective cell phenotypes of each population have been ascertained in our previous studies.[31,32,35,38,39] All media and supplements were purchased from Mediatech (Herndon, VA) except when otherwise noted.

Co-culture and tri-culture on multiphased scaffold

Co-culture of fibroblasts and osteoblasts on the triphasic scaffold was established following published methods.[31] Specifically, fibroblasts were cultured on Phase A of the scaffolds at a density of 5×10^5 cells/scaffold, followed by osteoblasts at a density of 2.5×10^5 cells/scaffold on Phase C. The fibroblast to osteoblast ratio was 2:1 due to the higher surface area of Phase A as determined by mercury porosimetry. After allowing each cell type to attach for 20 min, supplemented DMEM was added and the samples were incubated at 37°C under humidified conditions and 5% CO_2. Each well was pre-coated with agarose (Sigma, St. Louis, MO) in order to limit cell migration out of the scaffolds. The seeded scaffolds were cultured for 4 days prior to implantation.

To establish tri-culture of fibroblasts, chondrocytes and osteoblasts, Phase B of the scaffolds was first seeded with chondrocytes. Specifically, a chondrocyte suspension in 0.5% agarose was loaded into Phase B (5×10^5 cells/phase) and left to gel for 15 min. Fibroblasts and osteoblasts were subsequently seeded on Phase A and Phase C, respectively, following the methods described above.

In vivo model and surgical procedure

All surgical procedures[40–42] were performed in accordance with a protocol approved by the Institutional Animal Care and Use Committee (IACUC) at the Hospital for Special Surgery. A total of 27 male athymic rats (NIH-*rnu*, 225–250 g, Charles River Laboratories, Wilmington, MA) were used for this study, and the three experimental groups included tri-cultured, co-cultured, and acellular scaffolds. The animals were anesthetized with 4% isoflurane in high flow oxygen and by intraperitoneal injection of 90 mg/kg ketamine and 4 mg/kg xylazine. The animals were maintained under anesthesia using isoflurane (1–2%) administered through an oxygen mask. Up to four individual subcutaneous pouches (1.5 cm) were formed through single incisions made in the posterior dorsum of the animal. Each animal received three scaffolds, one each of the tri-cultured, co-cultured, and acellular groups, with scaffolds ~1 cm apart from neighboring scaffolds. For the sham control, nine animals were randomly selected to receive a fourth incision but no scaffold was implanted. The incisions were all closed with nylon sutures. Procaine penicillin (200,000 IU/kg) was administered intramuscularly once prior to surgery and then once daily for 3 days post-operatively. Analgesics were also administered immediately and at 12 h following surgery.

The animals were sacrificed at 2, 4, and 8 weeks post-implantation by carbon dioxide inhalation. The scaffolds were exposed post-mortem via C-shaped subcutaneous incisions peripheral to the scaffolds [Fig. 1(B)]. Dermal tissue was removed while maintaining a small segment of skin for identification of the dorsal and ventral sides of the scaffolds. Samples were subsequently prepared for analysis as described in the following sections.

Host tissue infiltration and scaffold cellularity

The effects of implantation on host tissue infiltration and cellularity of the triphasic scaffold were monitored over time. Collagen distribution in all three scaffold phases was assessed using the Modified Goldner's Masson Trichrome stain.[43] Briefly, the explanted scaffolds ($n = 2$/group) were fixed in 10% neutral buffered formalin for 48 h, then transferred to 0.01*M* cacodylate buffer (Sigma, St. Louis, MO) until analysis. The explants were decalcified in 5% formic acid and then processed for paraffin embedding (Tissue Tek VIP Tissue Processor, Sakura Finetek U.S.A., Inc., Torrance, CA). Sample sections (6 μm, Reichert-Jung RM 2030 Microtome, Leica, Bannockburn, IL) were used for standard histological or immunohistochemical analysis.

Cellularity ($n = 5$) was determined by quantifying total DNA per scaffold using the PicoGreen dsDNA assay (Molecular Probes) following the manufacturer's suggested protocol. Immediately after mechanical testing, the same scaffolds were treated with 0.1% Triton X-100 solution (Sigma, St. Louis, MO) and individually homogenized (Biospec, Bartlesville, OK). Sample fluorescence was measured with a microplate reader (Tecan, Research Triangle Park, NC), with excitation and emission wavelengths of 485 and 535 nm, respectively. The total number of cells in the sample was determined using the conversion factor of 8 pg DNA/cell.[44]

Maintenance of phase-specific matrix heterogeneity *in vivo*

The effects of implantation on the maintenance of phase-specific matrix distribution on the triphasic scaffold were evaluated. Specifically, deposition of proteoglycans, collagen types I, II, and III as well as mineral distribution on the triphasic scaffold were determined at 2, 4, and 8 weeks. Proteoglycan and collagen distribution was evaluated by histology and immunohistochemistry. Sulfated glycosaminoglycan (GAG) distribution in the scaffold was visualized with alcian blue stain.[22] The alcian blue staining solution pH was maintained at 1.0 in order to selectively stain the sulfate groups of the proteoglycans rather than the carboxyl groups on the PLGA.[45] Deposition of types I, II, III, and X collagen was evaluated by immunohistochemistry.[22] Specifically, monoclonal antibody against type I collagen (1:20 dilution) was purchased from Calbiochem, and monoclonal antibodies against type II collagen (1:20 dilution) and type X collagen (undiluted) were purchased

from Developmental Studies Hybridoma Bank (Iowa City, IA). Type III collagen monoclonal antibody (1:100 dilution) was purchased from Sigma (St. Louis, MO). Before staining for type II collagen, the sections were treated with 1% hyaluronidase for 30 min at 37°C. All sample sections were incubated with primary antibody overnight at 4°C. Following a wash with buffer, biotinylated secondary antibody and streptavidin conjugate (LSAB 2 system, DAKO, Carpinteria, CA) were added. Positive staining was indicated by the formation of red-brown precipitates.

Mineral distribution ($n = 2$) on the triphasic scaffolds was determined by micro-computed tomography (CT) analysis and histology. Briefly, the retrieved scaffolds ($n = 2$) were fixed in 10% neutral buffered formalin for 48 h and stored in 0.01 *M* cacodylate buffer until analysis. Scaffolds were first scanned by micro-CT (VivaCT 40, Scanco, Switzerland) with a slice increment of 21 μm and 500 projections/180°, then embedded in poly(methylmethacrylate) using a modification of the methods of Erben et al.[46] Mineralization in the scaffolds was also visualized by von Kossa staining.[47] The sections (10 μm) were covered in 5% silver nitrate solution and exposed to ultraviolet light for 20 min in order to initiate the reaction. The samples were then rinsed with water and viewed under light microscopy (Zeiss Axiovert 25, Zeiss, Germany).

Scaffold mechanical properties

The effects of *in vivo* implantation on scaffold mechanical properties were determined at 0, 4, and 8 weeks. Specifically, the explanted samples ($n = 5$) were tested under uniaxial compression (MTS 810, Eden Prairie, MN) following published methods.[31,34] Briefly, the scaffolds were compressed at a displacement rate of 1.3 mm/min following a 10 *N* preload. A stress–strain curve was generated and compressive modulus was determined by calculating the slope of the initial linear region of the stress-strain curve. Yield strength was calculated using a 0.2% strain offset from the initial linear region.

Statistical analysis

Results are presented in the form of mean ± standard deviation, with n equal to the number of samples analyzed. Two-way analysis of variance (ANOVA) was performed to determine the effects of co-culture and implantation time on scaffold compressive modulus and cell proliferation. Fisher's LSD post-hoc test was utilized for all pair-wise comparisons and statistical significance was attained at $p < 0.05$. All analyses were performed using the JMP statistical software package (SAS Institute, Cavy, NC).

RESULTS

Host infiltration, matrix cellularity, and remodeling

The animals remained healthy and infection-free throughout the study. In terms of host infiltration, abundant tissue ingrowth in all three phases of the scaffold was observed for the co-cultured and tri-cultured groups. This is evident in the series of Trichrome stains shown in Figure 1(C), with the collagenous matrix stained in green, erythrocytes in red, and cell nuclei in black. By week 4, an extensive collagen-rich matrix was prevalent in all three phases of the seeded scaffolds [Fig. 1(C)]. As shown in the higher magnification images taken of the center of each scaffold phase (Fig. 2), vascularized collagenous tissue readily infiltrated the pores surrounding the polymer fibers in Phase A, and was deposited between microspheres within Phase B and Phase C. In contrast, tissue infiltration into the scaffold was markedly reduced in the acellular group [Fig. 1(C)] and was limited to the periphery of the scaffold phases (Fig. 2).

By week 8, Phase A had degraded in all three groups, and tissue remodeling was evident as a drastic change in tissue morphology that was observed between weeks 4 [Fig. 1(C)] and 8 (Fig. 3). The co-cultured scaffold was enveloped by a loose connective tissue, while both the acellular and tri-cultured scaffold groups were surrounded by a dense, cellularized, collagen-rich tissue layer. Based on Trichrome staining, the most abundant matrix was observed in the tri-cultured scaffolds, followed by the co-cultured group. In addition, while tissue infiltration into the acellular scaffolds at week 8 was much more extensive than at week 4, it was not comparable to what was observed for the two cell-seeded groups (Fig. 3).

The number of cells in the three scaffold groups was also compared over time. As seen in Figure 4, cellularity increased after initial seeding in all groups at 4 weeks post-implantation. The number of cells was comparable in the co-cultured and tri-cultured scaffold groups. While the average values were higher than the acellular in both groups, this difference was not found to be statistically significant. A decrease in cell number was found in all groups between weeks 4 and 8, most likely due to tissue remodeling as well as rapid hydrolytic degradation and resorption of Phase A, although a higher cell number was consistently measured for the tri-cultured and co-cultured groups. These observations corresponded with the scaffold resorption and tissue remodeling observed through histological analysis from week 4 to week 8.

Maintenance of phase-specific matrix heterogeneity *in vivo*

Co-cultured scaffold with fibroblasts and osteoblasts

The collagenous matrix found within Phases A, B, and C of the co-cultured scaffolds was comprised

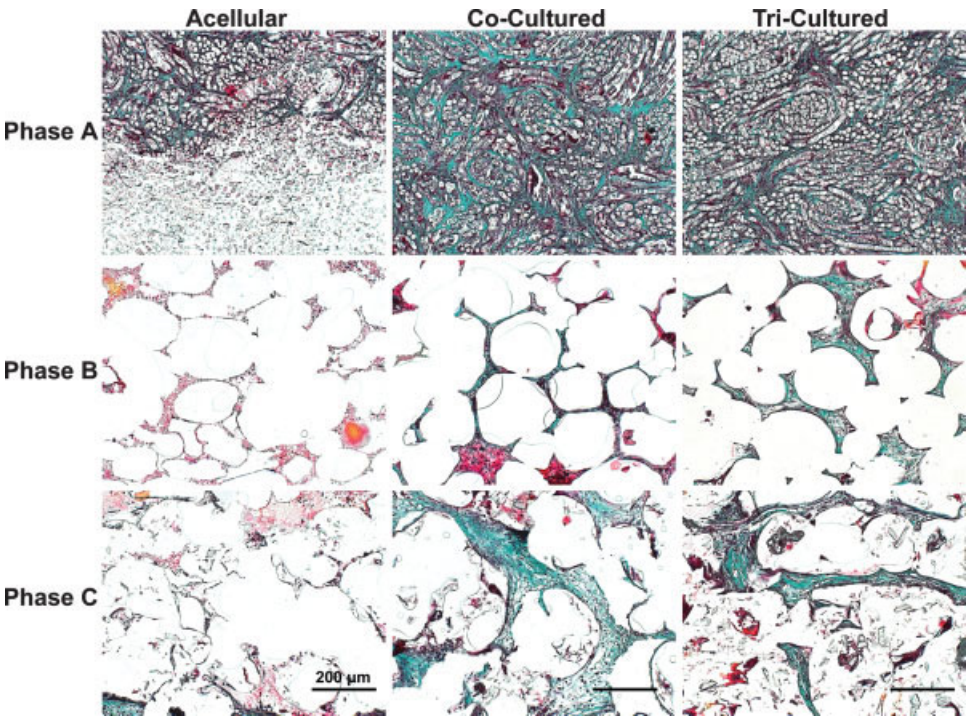

Figure 2. Matrix Distribution within the Multi-Phased Scaffold. Higher magnification images showing collagen production (green) in the center of each phase of the acellular (left), co-cultured (middle), and tri-cultured (right) scaffolds after 4 weeks of implantation. Tissue infiltration and extracellular matrix production were more abundant in the co-cultured and tri-cultured groups. (Modified Goldner's Masson Trichrome, week 4, 10×, bar = 200 μm).

primarily of type I collagen as indicated by immunohistochemistry at week 8 (Fig. 5). Type III collagen was found largely in Phase A of the scaffold. The co-cultured scaffold did not stain positive for fibrocartilage markers such as type II collagen and proteoglycans (data not shown). In addition, three-dimensional micro-CT reconstruction of mineral distribution showed that mineral was formed in Phase C of the scaffold, and that this mineralization was confined to this scaffold phase at all time points examined. Moreover, von Kossa staining confirmed the phase-specific mineral distribution (data not shown).

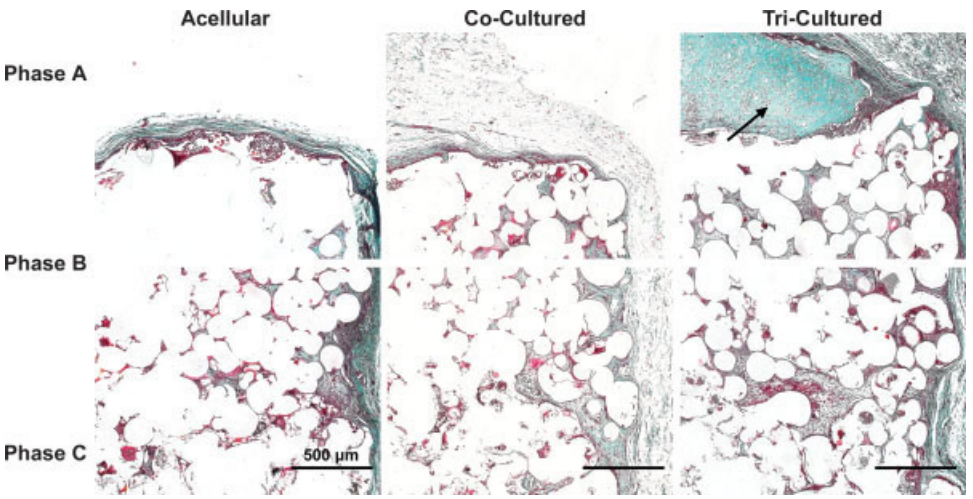

Figure 3. Collagen Production (green) in Multiphased Scaffolds. Tissue infiltration and extracellular matrix remodeling were observed to be greater in the co-cultured and tri-cultured groups after 8 weeks of implantation. Phase A has degraded and resorbed in all groups, with a fibrocartilage-like matrix observed in only the tri-cultured scaffolds (arrow). (Modified Goldner's Masson Trichrome, week 8, 5×, bar = 500 μm).

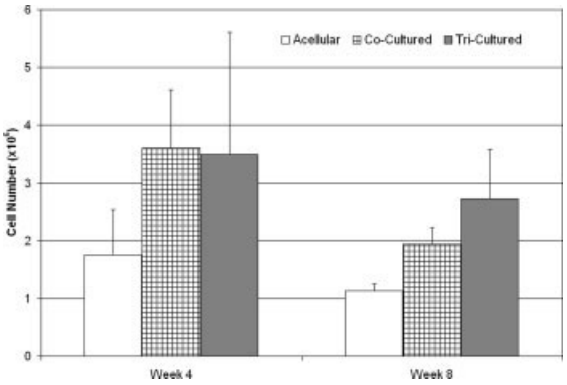

Figure 4. Cellularity of the Explanted Scaffolds. Cell number was higher in the seeded groups compared to the acellular group at both time points, with a generally decreasing trend in cell number over time, most likely due to tissue remodeling and degradation of Phase A of the scaffold ($p < 0.05$).

Tri-cultured scaffold with fibroblasts, chondrocytes, and osteoblasts

Similar to the co-cultured scaffold group, the matrix found in Phase A of the tri-cultured scaffolds also consisted of types I and III collagen at week 4. However, by week 8, after Phase A had degraded, a fibrocartilage-like region was found between Phase A and Phase B (Fig. 3, arrow). As seen in Figure 6, immunohistochemical analysis and alcian blue staining revealed positive staining for fibrocartilage markers such as types I and II collagen, as well as sulfated-proteoglycans (blue, Fig. 6) within this region. In addition, a localized region of type X collagen was detected (red-brown, Fig. 6). No comparable fibrocartilage-like region was observed in either the co-cultured or acellular groups.

For mineral distribution, micro-CT analysis revealed that, similar to the co-cultured and acellular groups, calcification was again confined to Phase C for the tri-cultured group [Fig. 7(A)]. The apparent mineral density was greater for the co-cultured and tri-cultured groups compared to the acellular control. Moreover, the phase-specific distribution of mineral content detected by micro-CT analysis was confirmed by von Kossa staining [black, Fig. 7(B)].

Scaffold integrity and mechanical properties

Uniaxial compression testing of the explanted scaffolds revealed an initial decrease in compressive modulus from week 0 to week 4 as expected [Fig. 8(A)]. This initial decrease was maintained in the acellular scaffold group. In contrast, an increase in compressive modulus occurred in the co-cultured and tri-cultured groups between weeks 4 and 8. A significant difference over time was detected in the co-cultured group ($p < 0.05$). The moduli obtained for the co-cultured and tri-cultured groups were consistently higher than that of the acellular control; however, this difference was not significant. For yield strength, there was a generally decreasing trend evident in all scaffold groups over the 8-week implantation period [Fig. 8(B)].

DISCUSSION

Our long-term goal is to facilitate biological fixation by engineering a functional interface between soft tissue grafts and subchondral bone. Combining a novel biomimetic scaffold design with spatial control of heterotypic cellular interactions between interface-relevant cell populations, the objective of this study is to determine the effects of the *in vivo* environment on the maintenance of the phase-specific matrix heterogeneity pre-formed through the co-culture of fibroblasts and osteoblasts, as well as the triculture of fibroblasts, chondrocytes, and osteoblasts. In particular, we examined whether distinct yet continuous matrix phases can be established on the scaffold in the complex *in vivo* environment, effectively evaluating the potential of the stratified scaffold for multitissue regeneration. It was found that the multiphased scaffold design and phase-specific distribution of fibroblasts, chondrocytes and osteoblasts resulted in the formation of a fibrocartilage-interface like tissue. In addition, phase-specific distribution of mineralized matrix corresponding to the bone region was established on the triphasic scaffold. These findings demonstrate the potential of the stratified scaffold to recapitulate the matrix distribution and organization inherent at the ligament-to-bone interface, which is critical for establishing a functional transition between the soft tissue graft and bone.

Stratified scaffold systems have been researched for orthopedic tissue engineering, and in particular for osteochondral applications.[48–53] Schaefer et al.[50] seeded bovine articular chondrocytes on PGA meshes and periosteal cells on PLGA/polyethylene glycol foams, and subsequently sutured these constructs together. Integration was observed to be superior when joined at one week, suggesting the importance of immediate cellular interactions. Similarly, Gao et al.[51] seeded mesenchymal stem cell-derived chondrocytes in a hyaluronan sponge, and osteoblasts in a porous calcium phosphate scaffold. These scaffolds were then joined by a fibrin sealant and implanted subcutaneously in syngeneic rats, with continuous collagen fibers observed between the two scaffolds at 6 weeks post-implantation. In addition, distinct cartilaginous and osseous zones were formed. In these pioneering studies of multi-

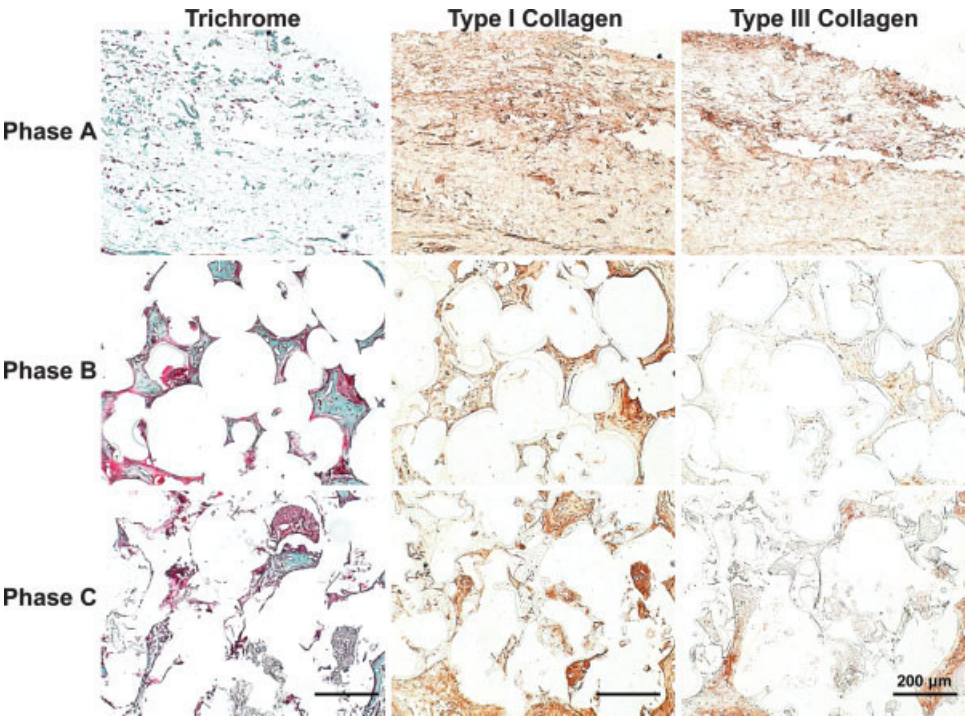

Figure 5. Collagen I and III Distribution in the Co-Cultured Scaffolds. Type I collagen was observed throughout all three phases of the scaffold, with positive staining for type III collagen localized largely in Phase A (Immunohistochemistry, week 8, 10×, bar = 200 μm).

tissue formation, scaffolds with either osteoblasts or chondrocytes were first cultured separately and then joined together. This process however minimizes the immediate cellular interactions necessary for eventual construct integration. In addition, scaffold integrity is not optimal in these reported scaffolds as the integration between the two phases is discontinuous. In contrast, the triphasic scaffold design utilized in

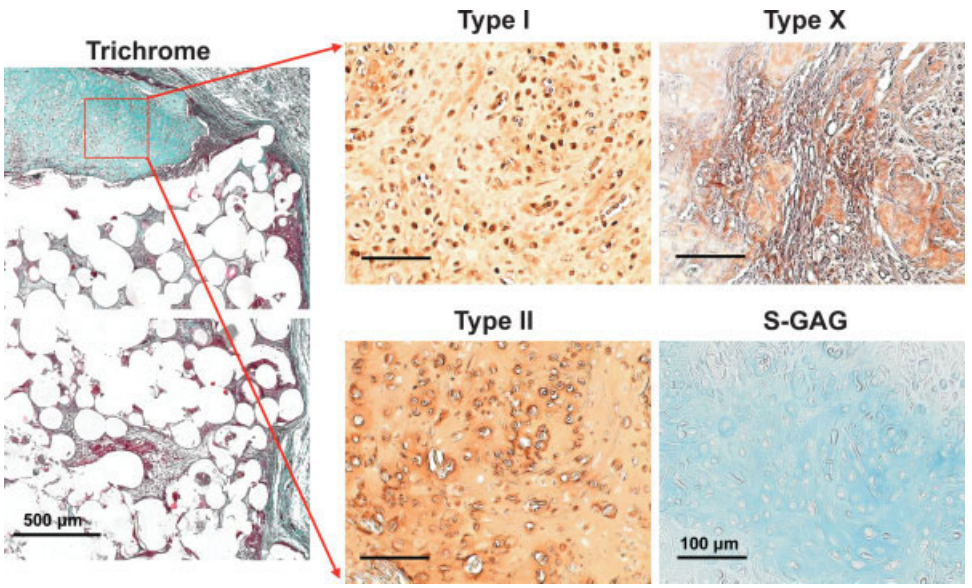

Figure 6. Formation of a fibrocartilage-like region in tri-culture. By week 8, a collagen-rich (green) and chondrocyte-containing matrix resembling the neonatal interface fibrocartilage was observed in only the tri-cultured group (left, Modified Goldner's Masson Trichrome, 5×, bar = 500 μm). This neo-fibrocartilage was comprised of types I and II collagen (red-brown) as well as glycosaminoglycans (S-GAG, blue). Localized production of type X collagen (red-brown) was also observed in the fibrocartilage region (20×, bar = 100 μm).

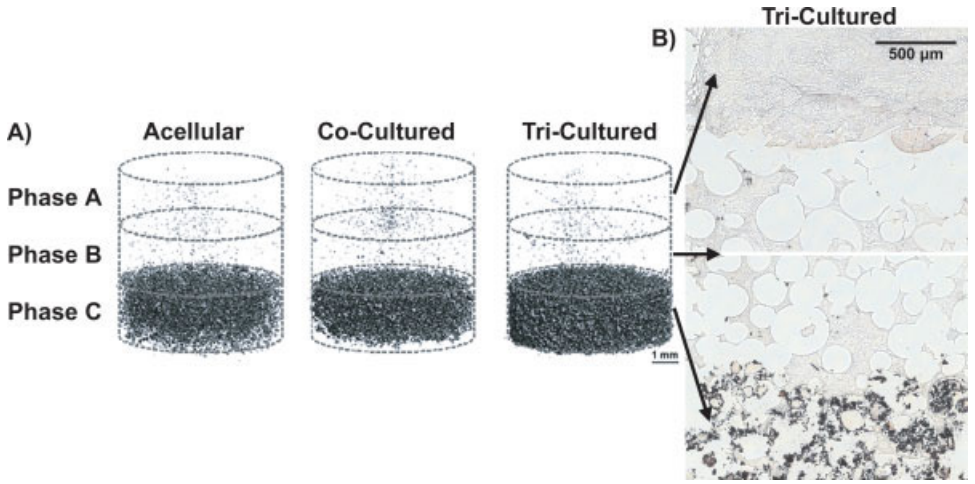

Figure 7. Phase-specific mineral distribution on the multiphased scaffold. Mineral presence and calcification was confined to Phase C for all scaffold groups as characterized by (A) Micro-CT and (B) von Kossa staining (Tri-cultured, week 4, 5×, bar = 500 μm). [Color figure can be viewed in the online issue, which is available at www.interscience.wiley.com.]

this study consists of a single continuous construct with integrated phases, upon which cells can interact immediately after seeding. Moreover, previous stratified scaffold designs focused primarily on the soft and hard tissue regions while neglecting the complex interface; the regeneration of which is essential for mediating load transfer between these two distinct tissue types and achieving biological fixation. Therefore, we have elected to incorporate an interface phase as well as the soft and hard tissue regions into the stratified scaffold design. By controlling the phase-specific distribution of fibroblasts, chondrocytes, and osteoblasts, multitissue formation has been engineered on the stratified scaffold both *in vitro* and *in vivo*. The fibrocartilage region formed in tri-culture exhibited characteristic markers such as types I and II collagen as well as proteoglycan production. Interestingly, both cell shape and matrix morphology of the neo-fibrocartilage resembled that of the neonatal fibrocartilage tissue observed at the ACL-bone insertion.[22]

As the triphasic scaffold is comprised of three distinct scaffold phases, which differed significantly in architecture, porosity, and composition, we also examined host tissue infiltration as well as the effect of *in vivo* culture on scaffold integrity and mechanical properties. It was found that the triphasic scaffold design supported host tissue ingrowth and cell-specific matrix production *in vivo*, with more abundant collagenous matrix found in the tri-cultured and co-cultured scaffold groups compared to the unseeded scaffold. As expected, compressive modulus decreased from week 0 to week 4 for all groups, attributed to the hydrolytic degradation of the polymer component of the scaffold. The observed initial decrease in modulus and yield strength is characteristic of bulk eroding polymers such as poly-α-hydroxyesters.[31,35,54,55] Interestingly, this expected

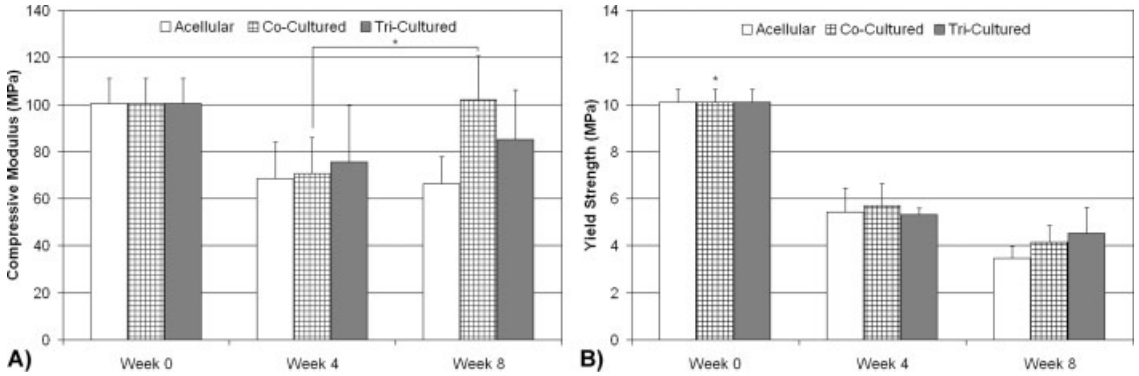

Figure 8. Effects of Implantation on Scaffold Mechanical Properties. (A) Compressive modulus decreased initially from week 0 to week 4, most likely due to polymer degradation. With extensive tissue infiltration and matrix production, the modulus increased in the tri-cultured and co-cultured groups at week 8 (*$p < 0.05$). (B) Scaffold yield strength decreased for all groups due to scaffold degradation *in vivo*.

decline in mechanical properties was followed by a significant increase in modulus for the co-cultured group at 8 weeks post-implantation. Mechanical properties of the seeded scaffolds were also consistently higher than those of the acellular control. These observations suggest that preseeding of the scaffold with connective tissue cells promoted host tissue infiltration and remodeling. More importantly, the abundant matrix elaboration and mineral formation observed in the seeded groups maintained scaffold integrity by compensating for scaffold degradation *in vivo*.

In this study, preculturing the scaffold phases with interface-relevant cells *in vitro* enhanced tissue infiltration and vascularization *in vivo*. These observations are in agreement with previously published studies,[56,57] in which cell-seeded scaffolds exhibited greater tissue production, cellular infiltration, and vascularization compared to acellular controls *in vivo*. Thornton et al.[56] implanted alginate scaffolds rehydrated with either bovine articular chondrocyte cell suspension or plain media into subcutaneous pouches of SCID mice. After 8 and 24 weeks, the seeded scaffolds exhibited superior mechanical properties and structural integrity compared to the acellular scaffolds.[56] Although the three cell types used in this study were not tracked, Bellincampi et al. investigated the effect of implantation site and cell type on cell longevity *in vivo* in a rabbit model.[57] It was reported that the autogenous fibroblasts seeded on collagen scaffolds were still present after 4–6 weeks *in vivo* regardless of implantation site, but more cells were detected within the subcutaneous pouch compared to the intra-articular model. Observations from the current study indicate that the interface-relevant cells preseeded on the scaffold remained viable and had a positive effect on tissue formation, as demonstrated by the enhanced matrix infiltration and production found for the seeded scaffolds compared to the acellular group. The viability of the seeded chondrocytes is further evidenced in the tri-cultured group, in which the implanted cells formed a fibrocartilage-like matrix after 8 weeks. In addition, similar to Thornton et al.,[56] scaffold seeding in this study compensated for scaffold degradation in terms of improved mechanical properties in the seeded groups compared to the acellular scaffolds. These observations collectively demonstrate the beneficial effects of preseeding tissue engineered scaffolds with cell types of interest. As such, the nature and magnitude of this *in vivo* response will likely depend on factors such as scaffold composition, implantation site, cell source, and the choice of immunocompetent versus immunodeficient animal models. Future studies will focus on evaluating the fate of the implanted interface-relevant cell types, and deciphering their relative contribution to the observed healing response.

It is noted here that the introduction of the triculture of fibroblasts, chondrocytes, and osteoblasts significantly increased the complexity of the triphasic scaffold system. Although loading chondrocytes into Phase B facilitated the formation of fibrocartilage-like matrix within the scaffolds at week 8, the cell-type and matrix distributions were not entirely phase-specific as the interface tissue was found between Phase A and Phase B rather than localized within the interface phase. It is likely that with the predesigned higher porosity of Phase A for soft tissue formation,[31] the chondrocyte-laden hydrogel may have penetrated into Phase A during seeding. Therefore, the triphasic scaffold design must be further optimized for spatial control of cell distribution, and this can be established by preincorporating nanofiber-based cell-migration barriers between the three phases. Studies are currently underway to evaluate the efficacy of the modified scaffold system in both *in vitro* and *in vivo* studies.[58] Moreover, interpretation of the results of this study must also take into consideration the animal model used. Although the athymic subcutaneous model is well established for evaluating tissue engineered grafts and is optimal for determining the effects of exercising spatial control of cell distribution on multitissue formation, the full *in vivo* host response is not observed, especially when compared to an intra-articular, immunocompetent model. Additionally, physiologically relevant loading is not experienced by the interface scaffold in the subcutaneous environment. Therefore, future studies will focus on evaluating the tri-cultured scaffold in an immunocompetent intra-articular model that will expose the scaffold to both host response and physiological loading.

It is envisioned that the triphasic scaffold can be used to guide the re-establishment of an anatomic fibrocartilage interfacial region directly on soft tissue grafts. Specifically, the scaffold can be used as a graft collar during ACL reconstruction surgery. It can be fabricated as a hollow cylinder through which the ACL graft will be inserted, seeded with interface relevant cells on each phase, and secured to the ends of the graft. Fixation is achieved by inserting the collar-graft complex into the bone tunnel, with Phases A and B remaining within the joint cavity. It is anticipated that controlled cellular interactions coupled with mechanical loading will promote the formation of a fibrocartilage region directly on the ACL reconstruction graft. The optimal scenario is to have a completely mineralized tendon in the bone tunnel, and a physiologically equivalent fibrocartilage insertion superficial to the bone. In addition, for functional ligament tissue en-

gineering, the triphasic scaffold may be coupled with synthetic ACL grafts either as a graft collar or preincorporated into degradable polymer-based ACL prostheses.[27] It is anticipated that by focusing on engineering soft tissue-to-bone integration *ex vivo*, the complexity of intra-articular graft reconstruction would be reduced to bone-to-bone integration *in vivo*. Moreover, the biomimetic scaffold design and multi-lineage cell culture methods described here will be applicable to the formation of other soft tissue-to-bone interfaces, as well as the development of complex musculoskeletal tissue systems with the potential for seamless integration with the host environment.

CONCLUSIONS

We have reported here on the *in vivo* evaluation of a novel triphasic scaffold for soft tissue graft-to-bone integration. This biomimetic stratified scaffold supported heterotypic cellular interactions *in vivo* and resulted in the formation of distinct yet continuous cellular and matrix regions. Additionally, scaffold design along with cell seeding promoted tissue infiltration and matrix production and remodeling. Moreover, cell type- and phase-specific matrix heterogeneity was maintained on the scaffold *in vivo*, with distinct mineral and fibrocartilage-like tissue regions. The results of this study demonstrate the feasibility of multitissue regeneration on a single graft, with the potential to promote biological fixation of soft tissue grafts to bone. Future studies will focus on scaffold optimization and *in vivo* scaffold evaluation in a physiologically relevant tendon-to-bone healing model.

The authors thank Dr. Andrés García of the Georgia Institute of Technology and Dr. David Kaplan of Tufts University for generously sharing their animal protocols, as well as Natalie Leong and Kristen Moffat for assistance with surgery and animal care.

References

1. Johnson RJ. The anterior cruciate: A dilemma in sports medicine. Int J Sports Med 1982;3:71–79.
2. Gordon MD, Steiner ME. Orthopaedic knowledge update: Sports medicine. In: Garrick JG, editor. Orthopaedic Knowledge Update: Sports Medicine. American Academy of Orthopaedic Surgeons: Rosemont, Illinois; 2004. p 169–181.
3. Owings MF, Kozak LJ. Ambulatory and inpatient procedures in the United States, 1996. Vital Health Stat 1998;13:1–119.
4. Noyes FR, Mangine RE, Barber S. Early knee motion after open and arthroscopic anterior cruciate ligament reconstruction. Am J Sports Med 1987;15:149–160.
5. Daniel DM, Stone ML, Dobson BE, Fithian DC, Rossman DJ, Kaufman KR. Fate of the ACL-injured patient. A prospective outcome study. Am J Sports Med 1994;22:632–644.
6. Tom JA, Rodeo SA. Soft tissue allografts for knee reconstruction in sports medicine. Clin Orthop 2002;402:135–156.
7. Barrett GR, Noojin FK, Hartzog CW, Nash CR. Reconstruction of the anterior cruciate ligament in females: A comparison of hamstring versus patellar tendon autograft. Arthroscopy 2002;18:46–54.
8. Beynnon BD, Johnson RJ, Fleming BC, Kannus P, Kaplan M, Samani J, Renstrom P. Anterior cruciate ligament replacement: Comparison of bone-patellar tendon-bone grafts with two-strand hamstring grafts. A prospective, randomized study. J Bone Joint Surg Am 2002;84A:1503–1513.
9. Rodeo SA, Suzuki K, Deng XH, Wozney J, Warren RF. Use of recombinant human bone morphogenetic protein-2 to enhance tendon healing in a bone tunnel. Am J Sports Med 1999;27:476–488.
10. Kurosaka M, Yoshiya S, Andrish JT. A biomechanical comparison of different surgical techniques of graft fixation in anterior cruciate ligament reconstruction. Am J Sports Med 1987;15:225–229.
11. Robertson DB, Daniel DM, Biden E. Soft tissue fixation to bone. Am J Sports Med 1986;14:398–403.
12. Cooper RR, Misol S. Tendon and ligament insertion. A light and electron microscopic study. J Bone Joint Surg Am 1970; 52:1–20.
13. Benjamin M, Evans EJ, Copp L. The histology of tendon attachments to bone in man. J Anat 1986;149:89–100.
14. Benjamin M, Evans EJ, Rao RD, Findlay JA, Pemberton DJ. Quantitative differences in the histology of the attachment zones of the meniscal horns in the knee joint of man. J Anat 1991;177:127–134.
15. Niyibizi C, Visconti CS, Kavalkovich K, Woo SL. Collagens in an adult bovine medial collateral ligament: Immunofluorescence localization by confocal microscopy reveals that type XIV collagen predominates at the ligament-bone junction. Matrix Biol 1995;14:743–751.
16. Niyibizi C, Sagarrigo VC, Gibson G, Kavalkovich K. Identification and immunolocalization of type X collagen at the ligament-bone interface. Biochem Biophys Res Commun 1996;222:584–589.
17. Sagarriga VC, Kavalkovich K, Wu J, Niyibizi C. Biochemical analysis of collagens at the ligament-bone interface reveals presence of cartilage-specific collagens. Arch Biochem Biophys 1996;328:135–142.
18. Wei X, Messner K. The postnatal development of the insertions of the medial collateral ligament in the rat knee. Anat Embryol (Berl) 1996;193:53–59.
19. Messner K. Postnatal development of the cruciate ligament insertions in the rat knee. Morphological evaluation and immunohistochemical study of collagens types I and II. Acta Anatomica 1997;160:261–268.
20. Petersen W, Tillmann B. Structure and vascularization of the cruciate ligaments of the human knee joint. Anat Embryol (Berl) 1999;200:325–334.
21. Thomopoulos S, Williams GR, Gimbel JA, Favata M, Soslowsky LJ. Variations of biomechanical, structural, and compositional properties along the tendon to bone insertion site. J Orthop Res 2003;21:413–419.
22. Wang IN, Mitroo S, Chen FH, Lu HH, Doty SB. Age-dependent changes in matrix composition and organization at the ligament-to-bone insertion. J Orthop Res 2006;24:1745–1755.
23. Woo SL, Buckwalter JA. AAOS/NIH/ORS workshop. Injury and repair of the musculoskeletal soft tissues. Savannah, Georgia, June 18–20, 1987. J Orthop Res 1988;6:907–931.
24. Friedman MJ, Sherman OH, Fox JM, Del Pizzo W, Synder SJ, Ferkel RJ. Autogeneic anterior cruciate ligament (ACL) anterior reconstruction of the knee. A review. Clin Orthop 1985; 196:9–14.

25. Jackson DW, Grood ES, Arnoczky SP, Butler DL, Simon TM. Cruciate reconstruction using freeze dried anterior cruciate ligament allograft and a ligament augmentation device (LAD). An experimental study in a goat model. Am J Sports Med 1987;15:528–538.
26. Yahia L. Ligaments and Ligamentoplasties. Springer Verlag: Berlin, Heidelberg; 1997.
27. Lu HH, Jiang J. Interface tissue engineering and the formulation of multiple-tissue systems. Adv Biochem Eng Biotechnol 2006;102:91–111.
28. Mikos AG, Herring SW, Ochareon P, Elisseeff J, Lu HH, Kandel R, Schoen FJ, Toner M, Mooney D, Atala A, Van Dyke ME, Kaplan D, Vunjak-Novakovic G. Engineering complex tissues. Tissue Eng 2006;12:3307–3339.
29. Moffat KL, Sun WA, Chahine NO, Pena PE, Doty SB, Ateshian GA, Hung CT, Lu HH. Characterization of the structure-function relationship at the ligament-to-bone interface. Procedings of the National Academy of Sciences 2008. In Press.
30. Spalazzi JP, Gallina J, Fung-Kee-Fung SD, Konofagou EE, Lu HH. Elastographic imaging of strain distribution in the anterior cruciate ligament and at the ligament-bone insertions. J Orthop Res 2006;24:2001–2010.
31. Spalazzi JP, Doty SB, Moffat KL, Levine WN, Lu HH. Development of controlled matrix heterogeneity on a triphasic scaffold for orthopedic interface tissue engineering. Tissue Eng 2006;12:3497–3508.
32. Wang IN, Shan J, Choi R, Oh S, Kepler CK, Chen FH, Lu HH. Role of osteoblast-fibroblast interactions in the formation of the ligament-to-bone interface. J Orthop Res 2007;25:1609–1620.
33. Borden M, Attawia M, Khan Y, Laurencin CT. Tissue engineered microsphere-based matrices for bone repair: Design and evaluation. Biomaterials 2002;23:551–559.
34. Lu HH, El Amin SF, Scott KD, Laurencin CT. Three-dimensional, bioactive, biodegradable, polymer-bioactive glass composite scaffolds with improved mechanical properties support collagen synthesis and mineralization of human osteoblast-like cells in vitro. J Biomed Mater Res 2003;64A: 465–474.
35. Lu HH, Cooper JA Jr, Manuel S, Freeman JW, Attawia MA, Ko FK, Laurencin CT. Anterior cruciate ligament regeneration using braided biodegradable scaffolds: *In vitro* optimization studies. Biomaterials 2005;26:4805–4816.
36. Spalazzi JP, Dionisio KL, Jiang J, Lu HH. Osteoblast and chondrocyte interactions during coculture on scaffolds. IEEE Eng Med Biol Mag 2003;22:27–34.
37. Mauck RL, Seyhan SL, Ateshian GA, Hung CT. Influence of seeding density and dynamic deformational loading on the developing structure/function relationships of chondrocyte-seeded agarose hydrogels. Ann Biomed Eng 2002;30:1046–1056.
38. Jiang J, Nicoll SB, Lu HH. Co-culture of osteoblasts and chondrocytes modulates cellular differentiation in vitro. Biochem Biophys Res Commun 2005;338:762–770.
39. Jiang J, Leong NL, Mung JC, Hidaka C, Lu HH. Interaction between zonal populations of articular chondrocytes suppresses chondrocyte mineralization and this process is mediated by PTHrP. Osteoarthr Cartil 2008;16:70–82.
40. Mauney JR, Jaquiery C, Volloch V, Heberer M, Martin I, Kaplan DL. *In vitro* and *in vivo* evaluation of differentially demineralized cancellous bone scaffolds combined with human bone marrow stromal cells for tissue engineering. Biomaterials 2005;26:3173–3185.
41. Byers BA, Guldberg RE, Garcia AJ. Synergy between genetic and tissue engineering: Runx2 overexpression and *in vitro* construct development enhance *in vivo* mineralization. Tissue Eng 2004;10:1757–1766.
42. Alhadlaq A, Mao JJ. Tissue-engineered neogenesis of human-shaped mandibular condyle from rat mesenchymal stem cells. J Dent Res 2003;82:951–956.
43. Gruber H. Adaptations of Goldner's Masson trichrome stain for the study of undecalcified plastic embedded bone. Biotech Histochem 1992;67:30–34.
44. Lu HH, Tang A, Oh SC, Spalazzi JP, Dionisio K. Compositional effects on the formation of a calcium phosphate layer and the response of osteoblast-like cells on polymer-bioactive glass composites. Biomaterials 2005;26:6323–6334.
45. Lev R, Spicer S. Specific staining of sulfate groups with Alcian Blue at low pH. J Histochem Cytochem 1964;12:309.
46. Erben RG. Embedding of bone samples in methylmethacrylate: An improved method suitable for bone histomorphometry, histochemistry, and immunohistochemistry. J Histochem Cytochem 1997;45:307–313.
47. von Kossa J. Ueber die im Organismus kunstlich erzeugen Verkalkungen. Beitr Path Anat 1901;29:163–202.
48. Lu HH, Jiang J, Tang A, Hung CT, Guo XE. Development of controlled heterogeneity on a polymer-ceramic hydrogel scaffold for osteochondral repair. Key Eng Mater (Bioceramics 17) 2005;17:607–610.
49. Yu H, Grynpas M, Kandel RA. Composition of cartilagenous tissue with mineralized and non-mineralized zones formed in vitro. Biomaterials 1997;18:1425–1431.
50. Schaefer D, Martin I, Shastri P, Padera RF, Langer R, Freed LE, Vunjak-Novakovic G. *In vitro* generation of osteochondral composites. Biomaterials 2000;21:2599–2606.
51. Gao J, Dennis JE, Solchaga LA, Awadallah AS, Goldberg VM, Caplan AI. Tissue-engineered fabrication of an osteochondral composite graft using rat bone marrow-derived mesenchymal stem cells. Tissue Eng 2001;7:363–371.
52. Hollister SJ, Maddox RD, Taboas JM. Optimal design and fabrication of scaffolds to mimic tissue properties and satisfy biological constraints. Biomaterials 2002;23:4095–4103.
53. Niederauer GG, Slivka MA, Leatherbury NC, Korvick DL, Harroff HH, Ehler WC, Dunn CJ, Kieswetter K. Evaluation of multiphase implants for repair of focal osteochondral defects in goats. Biomaterials 2000;21:2561–2574.
54. Chu CC. An in-vitro study of the effect of buffer on the degradation of poly(glycolic acid) sutures. J Biomed Mater Res 1981;15:19–27.
55. Thomson RC, Yaszemski MJ, Powers JM, Mikos AG. Fabrication of biodegradable polymer scaffolds to engineer trabecular bone. J Biomater Sci Polym Ed 1995;7:23–38.
56. Thornton AJ, Alsberg E, Hill EE, Mooney DJ. Shape retaining injectable hydrogels for minimally invasive bulking. J Urol 2004;172:763–768.
57. Bellincampi LD, Closkey RF, Prasad R, Zawadsky JP, Dunn MG. Viability of fibroblast-seeded ligament analogs after autogenous implantation. J Orthop Res 1998;16:414–420.
58. Spalazzi JP, Moffat KL, Lu HH. Design of a novel stratified scaffold for ACL-to-bone interface tissue engineering. 8th International Symposium on Ligaments and Tendons, 2008.